Combined Active Magnetic Bearing Topology to Control 3 Degrees of Freedom

Robert SANTNER*, Gerald JUNGMAYR*
*Linz Center of Mechatronics GmbH, Austria

Abstract

This paper proposes a compact topology for an active magnetic bearing (AMB) that integrates both radial and axial control into a single structure. A key innovation of the design is the use of a single bias magnet whose flux is shared between the axial and radial directions. At the same time, the active control flux paths remain separated, which is essential for implementing a simple and decoupled control concept. Moreover, the active flux does not pass through the bias magnet, allowing for strong active magnetic fields.

To evaluate the effectiveness of the proposed design, finite element simulations were performed using ANSYS Electronics. The combined bearing exhibits significantly less negative stiffness compared to separate radial and axial bearings, along with increased force-to-magnetomotive force ratios. To quantify this improvement, the *magnetic stiffness compensation coefficient* is introduced, relating these parameters to each other.

In addition to its magnetic performance, the design offers practical advantages: since the rotor is not mechanically interlocked with the bearing, it can be installed or removed without disassembling the bearing system. This makes the proposed solution especially attractive for high-speed and maintenance-sensitive applications.

Keywords: active magnetic bearing, combined topology, magnetic stiffness compensation coefficient, rotor levitation, bias flux, negative stiffness

1. Introduction

Active magnetic bearings (AMBs) enable contactless support of rotors by using magnetic forces, eliminating mechanical friction and wear. They are particularly advantageous in high-speed, vacuum, or sterile environments, where conventional bearings may fail or require frequent maintenance. However, most existing AMB systems require separate arrangements for axial and radial control with interlocking rotor and stator parts. This increases system complexity, physical size, and assembly effort.

In [2] an axial magnetic bearing has been proposed that can overcome the issue with interlocking parts. Together with radial bearings proposed in [1] a magnetic bearing system can be built that is well suitable for hight speed applications. Still, both designs suffer from increased negative stiffness effects due to unused return flux paths.

This paper presents a new AMB topology by combining the mentioned designs into one setup that unifies axial and radial stabilization. The main innovation lies in using a single bias magnet mounted on the rotor to provide the magnetization for both control directions. This results in a significant reduction in negative stiffness in both directions. At the same time, the active magnetic fluxes are decoupled and do not pass through the bias magnet.

A key mechanical benefit of the proposed design is that the rotor is not mechanically interlocked with the stator. This allows for quick and easy rotor installation and removal, without disassembling the magnetic bearing. Such a feature is particularly attractive in high-speed applications where serviceability is critical.

The remainder of this paper is organized as follows: Section 2 discusses the axial and radial magnetic bearings from [1] und [2] and introduces the novel combined bearing setups. Section 3 presents simulation results with a focus on negative stiffness, force-to-magnetomotive force (MMF) and introduces the magnetic stiffness compensation coefficient, section 4 discusses possible applications and section 5 summarizes the results.

2. Combined active magnetic bearing setup

The proposed combined active magnetic bearing (CMB) integrates two established configurations: one for radial and one for axial stabilization. The radial part is based on the design presented in [1], while the axial component follows the concept described in [2]. Both designs use bias flux in only one air gap to generate force, leaving the flux return path unused. This unused flux path contributes to increased negative stiffness.

2.1 Radial magnetic bearing

Figure 1 shows a sectional view of the radial magnetic bearing (RMB) described in [1]. The stator consists of the ferromagnetic stator yoke (1.1), four radial actuator coils (1.2), an axially magnetized permanent magnet ring (1.3), and an additional ferromagnetic yoke (1.4). The rotor includes a ferromagnetic core (1.5) and a non-ferromagnetic bandage (1.6). The bandage is not essential for functionality but may be required in a final prototype to assemble the rotor.

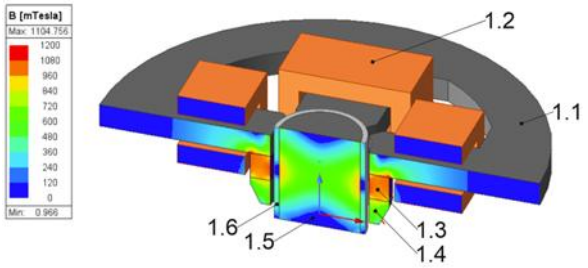

Figure 1 Section view of the radial magnetic bearing described in [1]

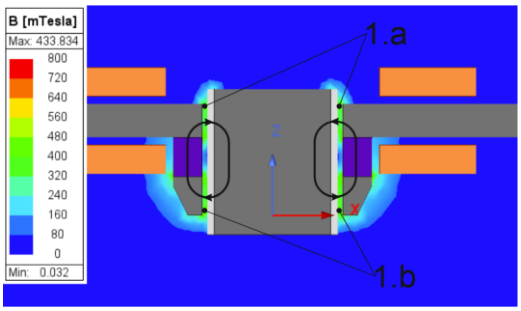

Figure 2: Magnetic bias flux density generated by the stator magnet

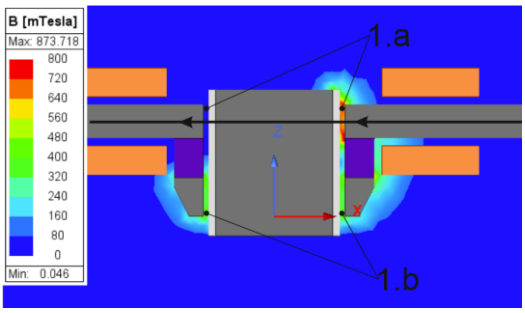

Figure 3: Resulting flux density with energized radial coils

Figure 2 illustrates the magnetic flux density in the air surrounding the components of the RMB. In this configuration, the flux is generated solely by the stator magnet, which provides the bias magnetization. The air gaps (1.a and 1.b) represent the entry and exit points of the flux into and out of the rotor. When the rotor is perfectly centred, the magnetic fields are symmetrical, and no net radial force acts on the rotor. However, the bias magnetization introduces negative stiffness—if the rotor is displaced slightly, magnetic forces will push it further away from the centre. This centred position is therefore an unstable equilibrium. Stronger magnetic fields in the air gaps result in greater negative stiffness and stronger destabilizing forces. The homogeneous circumferential magnetic field limits eddy current losses, making the RMB well suited for high-speed applications.

Figure 3 shows the magnetic field when a constant current is applied to the radial coils in this cross section. On the right side, the coil field and the bias field align, increasing the total magnetic field. On the left side, the fields oppose each other, weakening the magnetization. This imbalance creates a net radial force that pulls the rotor to the right.

Importantly, the bias flux in air gap 1.b is unaffected by the coil field and therefore does not contribute to force generation. However, it still increases the negative stiffness, making the system harder to control [3].

© 2025 The Japan Society of Mechanical Engineers

2.2 Thrust magnetic bearing

Figure 4 presents a sectional view of the thrust magnetic bearing (TMB) described in [2]. The stator consists of a ferromagnetic yoke (2.1) and an axial actuator coil (2.2). The rotor components include a permanently magnetized cylinder (2.4) with axial magnetization, a ferromagnetic yoke (2.3), an optional end cap for magnet protection (2.5), and a non-ferromagnetic bandage (2.6) to hold these parts together.

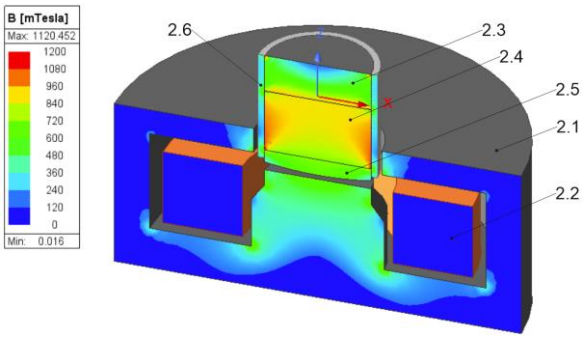

Figure 4: Section view of the axial magnetic bearing described in [2]

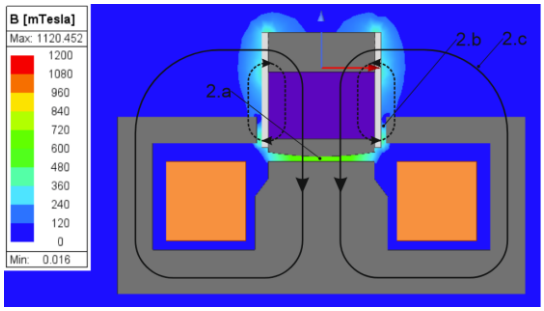

Figure 5: Magnetic bias flux density generated by the rotor magnet

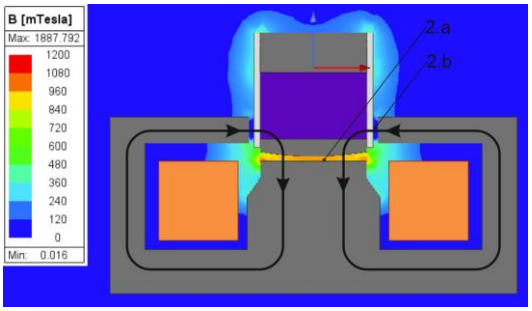

Figure 6: Resulting flux density with energized axial coil

Figure 5 shows the magnetic field of the TMB generated by the bias magnet mounted on the rotor. The solid line represents the main magnetic flux path: it crosses the axial air gap (2.a), follows the stator yoke, and returns to the magnet through the return path (2.c). This main flux path contributes to a negative axial stiffness, pulling the rotor downward. The dotted line represents a stray flux path, which crosses the radial air gap (2.b) and results in additional negative radial stiffness

Figure 6 illustrates the magnetic field when the axial coil is energized. The flux in the main air gap (2.a) increases, thereby increasing the axial force that pulls the rotor downward. Simultaneously, the flux in the radial air gap (2.b) decreases. Since this reduction is radially symmetric, it does not produce a net radial force; however, it does alter the radial stiffness.

This behaviour introduces an undesired coupling between the radial stiffness and the axial coil current. In practical terms, this is not a critical issue because the radial stability of the system must already be ensured by an additional radial bearing.

In essence, this TMB functions as an electromagnet that attracts or repels a permanent magnet mounted on the rotor. With the appropriate system design, this TMB can not only pull the rotor downwards but also generate forces upwards. This can be seen later in Figure 11. The bias magnetic flux pulls the rotor downwards when the TMB is not energized. This can be compensated by a constant current in the TMB or even better by an additional compensating negative stiffness, e.g. by another radial magnetic bearing.

© 2025 The Japan Society of Mechanical Engineers

2.3 Combined active magnetic bearing

Figure 7 shows the proposed CMB, designed to control three degrees of freedom. It integrates the previously described axial and radial components into a single compact system. The axial part remains largely unchanged. From the radial setup, only the ferromagnetic stator yoke (1.1) and the four radial actuator coils (1.2) are retained. The stator magnet (1.3) and yoke (1.4) are omitted, as the rotor-mounted magnet (2.4) now provides the bias magnetization for both radial and axial directions.

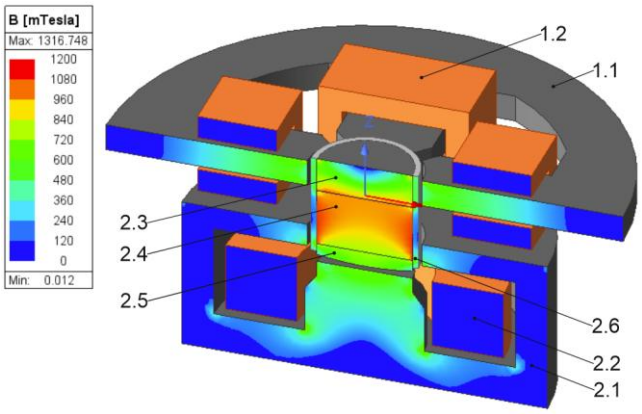

Figure 7: Section view of the proposed combined magnetic bearing

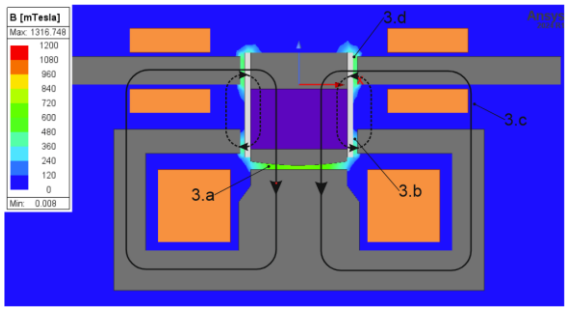

Figure 8: Magnetic bias flux density generated by the rotor magnet of the combined magnetic bearing

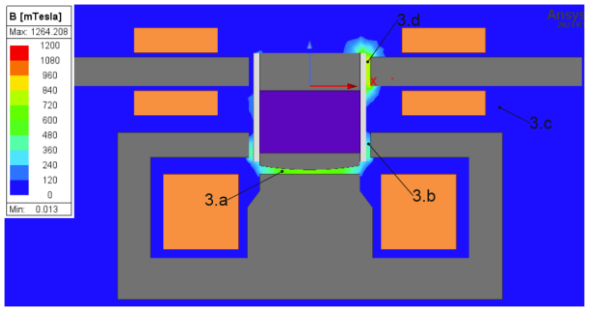

Figure 9: Resulting flux density with energized radial coils of the combined magnetic bearing

Figure 8 illustrates the magnetic bias flux paths in the combined setup, including both the main and stray flux components. The key advantage of this design becomes clear here: both the entry (3.a) and exit (3.d) air gaps of the main bias flux path are actively used to generate force. This improves efficiency and significantly reduces negative stiffness in both radial and axial directions.

In the radial direction, negative stiffness is reduced because the return path through air gap 1.b of the RMB (compare Figure 3) — which previously contributed to instability — is no longer present. In the axial direction, the main bias flux crosses the axial air gap (3.c), which is located entirely within stator-mounted components. Since this flux does not interact with the rotor, it does not generate any axial force. As a result, the overall negative axial stiffness is also reduced.

Figure 9 shows the magnetic field distribution when the radial coils are energized. On the right side of the rotor, the coil field and the bias field align, increasing the total magnetic flux on this side of air gap 3.d. On the left side, the fields oppose each other, reducing the flux. This asymmetry generates a net force that pulls the rotor to the right, achieving radial control.

The flux path generated by the axial coil remains unchanged from the path in Figure 6**: Resulting flux density with energized axial coil**. Thus, the active flux paths remain separated, which is key to a simple and decoupled control concept. At the same time, the active flux paths do not pass through the bias magnet, which leads to strong active magnetic fields. Both features boost the performance of this novel active magnetic bearing concept.

© 2025 The Japan Society of Mechanical Engineers

3. Simulation results

To evaluate the performance of the discussed bearing configurations, simulations were conducted using ANSYS Electronics. The resulting data was post-processed in MATLAB.

The characteristic dimensions used in all simulations are identical across the three bearing types to ensure comparability. These are listed below

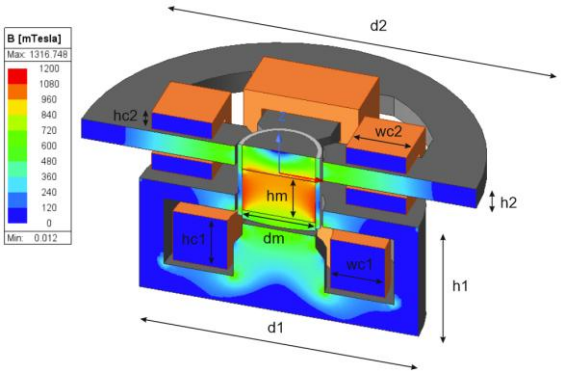

Figure 10: Characteristic dimensions of the CMB

Table 1: Characteristic dimensions

Dimension	Value
d1	46.0 mm
h1	20.0 mm
hc1	9.0 mm
wc1	9.0 mm
d2	65.0 mm
h2	3.5 mm
hc2	10.0 mm
wc2	3.0 mm
hm	7.5 mm
dm	12.0 mm

Figure 11 through Figure 14 illustrate the simulated behaviour of the three topologies. The current is specified in ampere windings (AW). This is the sum of the currents in each winding of the corresponding coil. With this metric, the characteristics shown do not depend on the winding design. In all cases, the force-displacement-current relationship appears approximately linear, which simplifies modelling and control.

Figure 11 shows the axial force of the TMB acting on the rotor as a function of both axial displacement and coil current. Even at zero current and zero displacement, a downward force of approximately 9.6 N is observed due to the bias magnetization. Nevertheless, this thrust bearing is still capable of generating positive (upward) forces.

Figure 12 presents the radial force characteristics of the RMB. The force is plotted against radial displacement and current. Because the setup is axially symmetric, only a one-sided deflection was simulated. The opposing side would exhibit the same behaviour with a reversed force direction.

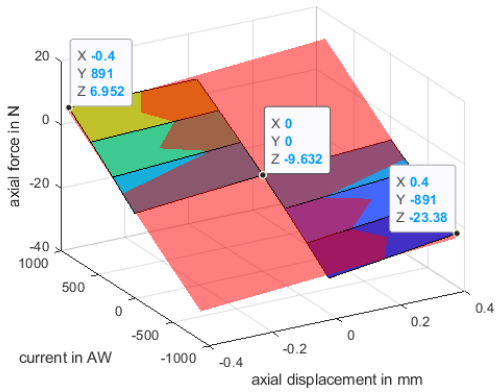

Figure 11: Axial force-displacement-current relationship of the TMB

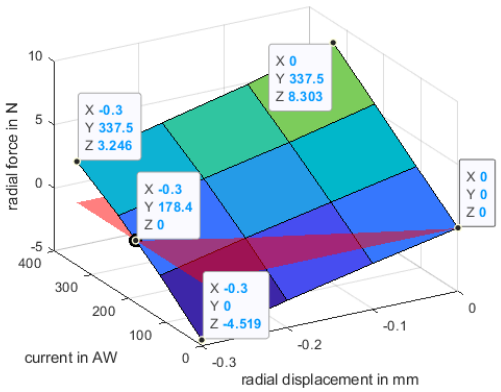

Figure 12: Radial force-displacement-current relationship of the RMB

© 2025 The Japan Society of Mechanical Engineers

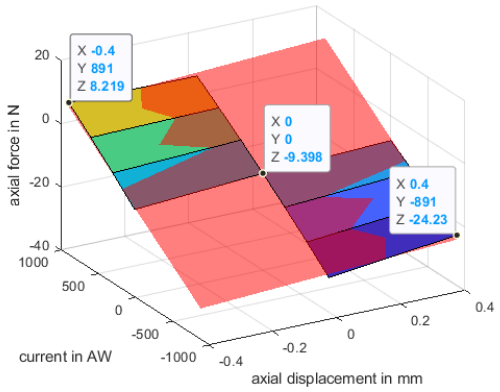

Figure 13: Axial force-displacement-current relationship of the CMB

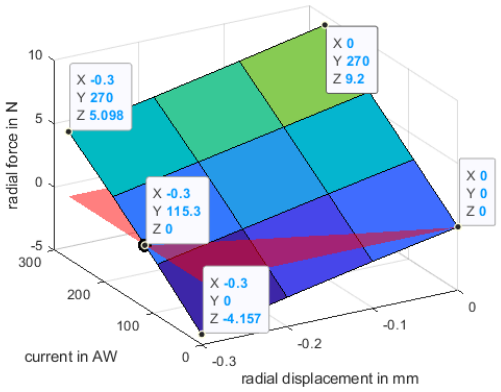

Figure 14: Radial force-displacement-current relationship of the CMB

The graphs in Figure 13 and Figure 14 show the axial and radial force characteristics of the combined magnetic bearing. The response appears quite linear and, at first glance, similar to the performance of the standalone axial and radial bearings. But a closer look at stiffness and force-to-magnetomotive force (MMF) ratios reveals the supreme performance of the combined design.

3.1 Magnetic stiffness compensation coefficient

To quantify the characteristics of the magnetic bearings, the stiffness values in radial and axial directions (k_x , k_z , in [N/mm]) and the corresponding force-to-MMF ratios ($k_{\theta x}$, $k_{\theta z}$, in [N/AW]) were calculated. These parameters allow for estimating the magnetomotive force (MMF) required to compensate the inherent negative stiffness when the rotor is displaced.

The ratio of stiffness to force-to-MMF in each direction defines the magnetic stiffness compensation coefficient:

$$\mathbf{c_x} = \frac{\mathbf{k_x}}{\mathbf{k_{\theta x}}} \quad , \mathbf{c_z} = \frac{\mathbf{k_z}}{\mathbf{k_{\theta z}}} \tag{1}$$

The unit of this coefficient is [AW/mm], indicating the amount of MMF required per millimetre of displacement to counteract the effect of negative stiffness. Multiplying this coefficient by a specific displacement yields the MMF needed to achieve compensation at that position.

The following table provides the mentioned parameters for the AMB designs under consideration.

Table 2:Characteristic parameters of the considered AMB designs

axial bearing:	radial bearing:
k_z = -7.3 N/mm	k_x = -15 N/mm
$k_{\theta z}$ = 20×10^{-3} N/AW	$k_{\theta x}$ = 25×10^{-3} N/AW
c_z = -365 AW/mm	c_x = -600 AW/mm

combined bearing axial:	combined bearing radial:
k_{zc} = -5.6 N/mm	k_{xc} = -13.9 N/mm
$k_{\theta xc}$ = 21×10^{-3} N/AW	$k_{\theta xc}$ = 34×10^{-3} N/AW
c_{zc} = -267 AW/mm	c_{xc} = -409 AW/mm

These results show a clear improvement with the combined topology.

In the axial direction, the compensation coefficient c_{zc} is 27% lower than that of the standalone axial bearing c_z.

→ Only 73% of the original MMF is needed to neglect negative stiffness.

In the radial direction, the compensation coefficient c_{xc} is 32% lower than in the standalone radial bearing c_x.

→ Only 68% of the original MMF is needed for stabilization.

© 2025 The Japan Society of Mechanical Engineers

These reductions indicate that the proposed combined bearing design improves controllability by significantly lowering the active current required to maintain rotor position.

This also affects the amount of current that is necessary to lift the rotor from the mechanic stop. Assuming the radial stops are at -0.3 mm the black points in Figure 12 and Figure 14 highlight the compensating MMF.

4. Applications

The magnetic bearing configurations presented in this paper are particularly well-suited for applications involving high-speed rotors. By using the proposed combined magnetic bearing together with an additional radial bearing, the rotor can be fully levitated without any mechanical interlocks. This feature offers a significant advantage in terms of maintenance and assembly.

The rotor can be installed or removed without disassembling either the combined magnetic bearing or the rotor itself. This makes the system especially attractive for applications where:

- Minimal downtime is required,
- Frequent rotor changes are needed,
- Space constraints limit accessibility for disassembly.

In such scenarios, the contactless and easily detachable design of the combined bearing can reduce system complexity, improve reliability, and lower operational costs. Additionally, the reduced magnetic stiffness compensation coefficient improves the controllability of the system.

5. Summary

This paper introduced a novel magnetic bearing topology that combines two known setups from [1] and [2]. By integrating radial and axial magnetic bearings into a single structure, the design minimizes negative stiffness in both directions. Simulation results confirm that the combined configuration reduces the required compensating MMF by up to 32% compared to standalone TMB or RMB.

Additionally, the proposed design simplifies mechanical integration compared to traditional AMBs, as it does not require physical interlocks between the rotor and stator. This enables easy rotor replacement and offers significant advantages for high-speed, maintenance-sensitive applications.

Overall, the combined magnetic bearing provides both improved control performance and practical benefits in system design and operation.

6. Acknowledgement

This work was carried out at LCM GmbH as part of a K2 project. K2 projects are financed using funding from the Austrian COMET-K2 program. The COMET-K2 projects at LCM are supported by the Austrian federal government, the federal state of Upper Austria, Johannes Kepler University Linz, and all partners that form part of the COMET-K2 consortium.

References

[1] Rieter CZ s.r.o., „Magnetlager, Welle und Wellenlagerung“ German Patent DE102014104531A1

[2] G. Jungmayr, H. J. Berroth, M. Panholzer, E. Marth, W. Amrhein, F. Jeske M. Reisinger, “Design of a Highly Reliable Fan with Magnetic Bearings”, Proceedings of ISMB14, pp. 42-47, 2014.

[3] G. Jugmayr, R. Santner, D. Freller, R. Netrval, L. Roberts, A. Ejlli, G. Mueller, „Design Aspects for a High-Precision Active Magnetic Bearing System”, Proceedings of ISMB19

© 2025 The Japan Society of Mechanical Engineers